

Finite-size effects in BaTiO₃ nanowires

Grégory Geneste¹, Eric Bousquet¹, Javier Junquera² and Philippe Ghosez¹

¹ *Département de Physique, Université de Liège, Bâtiment B-5, B-4000 Sart Tilman, Belgium*

² *CITIMAC, Universidad de Cantabria, Avda. de los Castros s/n, E-39005, Santander, Spain*

The size dependence of the ferroelectric properties of BaTiO₃ nanowires is studied from first-principles. We show that the ferroelectric distortion along the wire axis disappears below a critical diameter of about 1.2 nm. This disappearance is related to a global contraction of the unit cell resulting from low atomic coordinations at the wire surface. It is shown that a ferroelectric distortion can be recovered under appropriate tensile strain conditions.

Ferroelectric oxides constitute an important class of multifunctional compounds, attractive for numerous technological applications¹. Pushed by the miniaturization constraints imposed by future devices, there is now an increasing interest in the synthesis and use of nanosized ferroelectrics². Nowadays, various ferroelectric nanostructures – ultrathin films^{3,4}, nanowires⁵, nanotubes^{6,7}, nanoislands⁸ – can be grown with control at the atomic scale. However, bringing ferroelectrics to the nanoscale raises fundamental questions.

Ferroelectricity is a collective effect, resulting from a delicate balance between short-range and long-range Coulomb interactions. In confined structures, both interactions are modified with respect to the bulk and it is commonly believed that ferroelectricity is altered and eventually totally suppressed when the system reaches a critical size sometimes referred to as the “ferroelectric correlation volume”¹. First-principles simulations are a fundamental tool to understand size effects in ferroelectrics⁹. Recent first-principles studies provided valuable insight into the behavior of thin films and highlighted the crucial role of the depolarizing field^{10,11,12}. A few works based on effective Hamiltonians^{13,14} and shell models¹⁵ also considered other low dimensional systems, such as nanorods and nanodisks. However, despite these efforts, very little is known on the evolution of ferroelectric properties in nanowires with respect to their size and shape.

In this letter, we investigate from first-principles the influence of finite-size effects on the ferroelectric properties of BaTiO₃ nanowires. We identify a critical diameter below which the ferroelectric distortion along the wire axis is totally suppressed. We assign this behavior to surface atomic relaxation effects. Below the critical diameter, a ferroelectric state can be recovered under appropriate tensile strain conditions. The crucial role of the longitudinal interatomic coupling along Ti–O chains and the weak interchain interactions are also discussed.

We focus on stoichiometric infinite BaTiO₃ nanowires. As illustrated in Fig. 1, we consider model systems built from individual BaTiO₃ clusters that are assembled into infinite chains, themselves combined into wires of increasing diameters. These stoichiometric wires have two BaO and two TiO₂ lateral surfaces, as displayed in Fig. 1(d). This asymmetry is responsible for a dipole perpendicular to the wire axis. However, it will not be further discussed since it is not relevant to the present study¹⁶. In what fol-

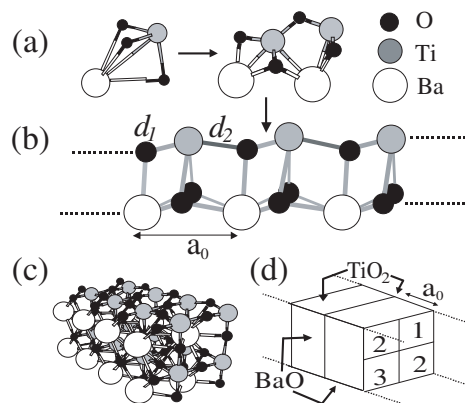


FIG. 1: (Color online) BaTiO₃ stoichiometric wires: BaTiO₃ clusters (a) assemble into infinite chains (b), themselves gathered into nanowires (c). The diameter of the nanowires is defined from the number of Ti–O chains (n) assembled together within the wire. Panels (c) and (d) correspond to $n = 4$.

lows, we will focus on the eventual disappearance of the ferroelectric instability *along* the wire direction z . The equilibrium lattice parameter along z will be referred to as a_0 , and the wire diameter will be specified by an integer n that corresponds to the number of Ti–O chains that are gathered together within the wire. The alternating Ti–O distances along z will be called d_1 and d_2 , as shown in Fig. 1(b).

Our calculations have been performed within the local density approximation (LDA) to density functional theory (DFT) using a numerical atomic orbital method as implemented in the SIESTA code¹⁷. Technical details are similar to those of Ref. 18. Some of the calculations have been double checked using the ABINIT package¹⁹. Periodic replicas of the wires are separated by more than 10 Å of vacuum. We explicitly checked that the replica of the wire generated by periodic boundary conditions is not affecting our results²⁰. The atomic positions have been relaxed until the maximum component of the force on any atom is smaller than 0.01 eV/Å.

For the thinnest wire ($n = 1$, Fig. 1(b)) the bond lengths and the equilibrium lattice constant a_0 of the relaxed structure reported in Table I are significantly shorter than in bulk. This can be explained from the low coordination of the different atoms in the structure,

TABLE I: Interatomic distances and equilibrium lattice parameter a_0 along the wire axis, for the $n = 1$ wire. O_I (resp. O_{II}) refers to oxygen atoms along the Ti-O (resp. Ba-O) chains. Results for the bulk cubic paraelectric unit cell of BaTiO_3 are shown for comparison. Units in Å.

	Ti- O_I	Ba- O_{II}	Ba-Ti	a_0
Wire	1.88	2.52	3.07	3.60
Bulk	1.97	2.78	3.41	3.94

the lack of some interactions being compensated by the strengthening of the remaining bonds. The system remains insulating with a bandgap of 3.3 eV. The relaxed structure presents a plane of symmetry perpendicular to z ($d_1 = d_2$) and is therefore not spontaneously polarized along the wire direction, demonstrating that ferroelectricity has disappeared. However, imposing a tensile strain, we can recover a polar structural distortion along the Ti-O chains ($d_1 \neq d_2$) above a critical lattice constant $a_c = 4.05$ Å. This strain induced phase transition is second order. Above a_c , both $d_1 - d_2$ and the polarization, calculated from the Berry phase approach,^{21,22} increase linearly with a_0 .

The fully relaxed $n = 4$ wire, shown in Fig. 1(c), is also non-polar along z . However, a_c has been reduced to 3.88 Å and a_0 is now larger (3.80 Å) as expected from the increase of the mean atomic coordination numbers with respect to the $n = 1$ wire. Figure 2 represents the evolution of a_0 and a_c for wires of increasing n . We observe that the difference, $a_c - a_0$, progressively decreases. A crossover between both curves is observed at $n_c = 9$, that corresponds to a diameter of 1.2 nm. Above n_c , unconstrained wires are ferroelectric whereas below this value, a spontaneous polarization only appears under tensile strain.

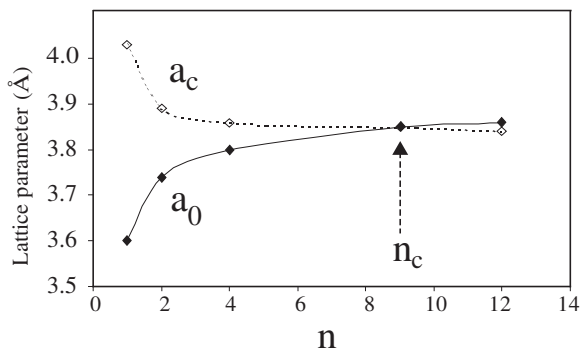


FIG. 2: Evolution of a_c (white diamonds) and a_0 (black diamonds) as a function of the number n of Ti-O chains in a transverse section of the wire.

In Fig. 2, a_c keeps a nearly constant value around 3.85 Å (except for $n = 1$) while the disappearance of the ferroelectric distortion at small sizes originates from

the progressive decrease of a_0 . The ferroelectric behavior of nanowires appears therefore to be monitored by the strong sensitivity of ferroelectricity to the unit cell volume, the latter affected by low coordination effects at free surfaces. As n increases, we recover a polar distortion, however, its amplitude only progressively increases as a_0 slowly evolves to its bulk value.

Similarly, below n_c , a second-order phase transition to a polar state is observed under tensile strain, but the resulting polarization strongly depends on the lattice parameter. This is illustrated in Fig. 3 for $n = 4$, where we quantify the polar distortion through the anisotropy of the interatomic distances ($d_2 - d_1$) along the distinct Ti-O chains. This provides a qualitative measure of the contributions to the polarization of the individual chains since the Born effective charges (along z) are reasonably similar from one chain to the other (variations smaller than 20 %²³). The strong inhomogeneity of the distortions for the different Ti-O chains highlights a deep influence of the surface: the ferroelectric distortion parallel to the wire surface is enhanced at TiO_2 surfaces and reduced around the BaO surfaces, a feature similar to what was previously reported for free-standing slabs²⁴. Note that the transition to the polar state does not occur at the same lattice constant in the different chains, giving rise, within a given range of lattice constants, to mixed ferroelectric-paraelectric states in these nanosized systems.

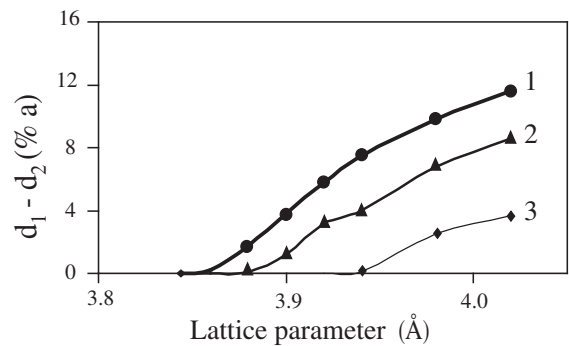


FIG. 3: Local distortions as a function of the lattice parameter for the $n = 4$ wire. Labels of the chains as in Fig. 1(d).

The distinct behavior of the different Ti-O chains within the same wire suggests weak inter-chain interactions. This is further confirmed by the fact that the polarization of each chain can be reversed almost independently, with very small changes in the total energy of the system and in the amplitude of the polar displacements. It is the longitudinal coupling of the atomic displacements inside individual Ti-O chains that appears as the main origin of the ferroelectric distortion. This behavior is similar to what was previously reported for the bulk²⁵. In the phonon dispersion curves of BaTiO_3 ²⁶, the unstable ferroelectric mode at Γ remains similarly unstable at X and M but *not* at R , pointing out a strong anisotropy of the interatomic force constants²⁵, a significant cou-

pling of the atomic displacement along Ti–O chains, and the absence of strong interchain interactions. The resulting "chain-like" character of the ferroelectric instability is intrinsic to BaTiO₃. It is preserved in nanowires and provides a general argument to understand the survival of ferroelectricity along the wire axis down to very small radii. The situation might be different in other compounds such as PbTiO₃ in which the ferroelectric instability is more isotropic²⁶.

In summary, the ferroelectric behavior of infinite stoichiometric BaTiO₃ nanowires has been studied from first-principles. In BaTiO₃, the ferroelectric instability exhibits a marked "chain-like" character so that, in nanowires, it could a priori be preserved down to very small sizes. Nevertheless, at small radii, low atomic coordinations at the surface produce a contraction of the

unit cell that is responsible for the suppression of the ferroelectric distortion at a critical radius estimated around 1.2 nm. Below this radius the ferroelectric distortion has disappeared at the equilibrium volume but can be recovered under appropriate tensile strain conditions.

Acknowledgements

The authors thank M. Dawber for careful reading of the manuscript. This work was supported by the VolkswagenStiftung (I/77 737), FNRS-Belgium (2.4562.03), the Région Wallonne (NOMADE) and the European Network of Excellence "FAME".

-
- ¹ M. E. Lines and A. M. Glass, "Principles and applications of ferroelectrics and related materials" (Clarendon Press, Oxford, 1977).
 - ² C. H. Ahn, K. M. Rabe, and J.-M. Triscone, *Science* **303**, 488 (2004).
 - ³ T. Tybell, C. H. Ahn, and J.-M. Triscone, *Appl. Phys. Lett.* **75**, 856 (1999).
 - ⁴ D. D. Fong, G. B. Stephenson, S. K. Streiffer, J. A. Eastman, O. Auciello, P. H. Fuoss, C. Thompson, *Science* **304**, 1650 (2004).
 - ⁵ W. S. Yun, J. J. Urban, Q. Gu, and H. Park, *Nano Lett.* **2**, 447 (2002).
 - ⁶ Y. Luo, I. Szafraniak, N. Zakharov, V. Nagarajan, M. Steinhart, R. B. Wehrspohn, J. H. Wendorff, R. Ramesh, M. Alexe, *Appl. Phys. Lett.* **83**, 449 (2003).
 - ⁷ F. D. Morrison, L. Ramsay, and J. F. Scott, *J. Phys.: Condens. Matter* **15**, L527 (2003).
 - ⁸ M. W. Chu, I. Szafraniak, R. Scholz, C. Harnagea, D. Hesse, M. Alexe, U. Gösele, *Nature Materials* **3**, 87 (2004).
 - ⁹ Ph. Ghosez and J. Junquera, in "Handbook of theoretical and computational nanotechnology", ed. M. Reith and W. Schommers (American Scientific Publishers, 2006), vol. 7, ch. 134 (to be published).
 - ¹⁰ J. Junquera and Ph. Ghosez, *Nature (London)* **422**, 506 (2003).
 - ¹¹ M. Dawber, K. M. Rabe and J. F. Scott, *Rev. Mod. Phys.* **77**, 1083 (2005).
 - ¹² I. Kornev, H. Fu, and L. Bellaiche, *Phys. Rev. Lett.* **93**, 196104 (2004).
 - ¹³ H. Fu and L. Bellaiche, *Phys. Rev. Lett.* **91**, 257601 (2003).
 - ¹⁴ I. Naumov, H. Fu, L. Bellaiche, *Nature (London)* **432**, 737 (2004).
 - ¹⁵ M. G. Stachiotti, *Appl. Phys. Lett.* **84**, 251 (2004).
 - ¹⁶ Similar calculations were performed for selected non-stoichiometric wires with full Ba-O and full TiO₂ coverage, yielding results similar to Fig. 2 except that the crossing between a_c and a_0 curves was slightly shifted to larger (resp. smaller) cell parameters for BaO (resp. TiO₂) coverage.
 - ¹⁷ J. M. Soler, E. Artacho, J. Gale, A. Garcia, J. Junquera, P. Ordejón, D. Sánchez-Portal, *J. Phys.: Condens. Matter* **14**, 2745 (2002).
 - ¹⁸ J. Junquera, M. Zimmer, P. Ordejón and Ph. Ghosez, *Phys. Rev. B* **67**, 155327 (2003).
 - ¹⁹ X. Gonze, J.-M. Beuken, R. Caracas, F. Detraux, M. Fuchs, G.-M. Rignanese, L. Sindic, M. Verstraete, G. Zerah, F. Jollet, M. Torrent, A. Roy, M. Mikami, Ph. Ghosez, J. -Y. Raty, D. C. Allan, *Computational Materials Science* **25**, 478 (2002); [URL: www.abinit.org].
 - ²⁰ To test the possible influence (especially in reason of the lateral dipole) of the artificial replica induced by the periodic boundary conditions, we repeated some calculations enlarging the vacuum regions up to 20 Å, without significant change in the results.
 - ²¹ R. D. King-Smith and D. Vanderbilt, *Phys. Rev. B* **47**, 1651 (1993).
 - ²² D. Sánchez-Portal, I. Souza, and R. M. Martin, in *Fundamental Physics of Ferroelectrics 2000*, edited by R. E. Cohen, AIP Conf. Proc. **535** (AIP, Melville, NY, 2000), p. 111.
 - ²³ The Born effective charges along z for the four Ti in a section of the wire of Fig. 1(c) are: $Z_{Ti1}^* = 5.10$, $Z_{Ti2}^* = 5.78$, $Z_{Ti3}^* = 5.93$ (labels as in Fig. 1(d)).
 - ²⁴ J. Padilla and D. Vanderbilt, *Phys. Rev. B* **56**, 1625 (1997).
 - ²⁵ Ph. Ghosez, X. Gonze, and J.-P. Michenaud, *Ferroelectrics* **206**, 205 (1998).
 - ²⁶ Ph. Ghosez, E. Cockayne, U. V. Waghmare, and K. M. Rabe, *Phys. Rev. B* **60**, 836 (1999).